Peer-reviewed version available at *Electronics* **2018**, *7*, 61; doi:10.3390/electronics7050061

Article

Bagged Decision Trees Based Scheme of Microgrid Protection Using Windowed Fast Fourier and Wavelet Transforms

Solomon Netsanet [1,*], Jianhua Zhang [1] and Dehua Zheng [2]

[1] School of Electrical & Electronic Engineering, North China Electric Power University, Beijing, China
[2] Goldwind Sc. & Tech. Co. Ltd, Beijing, China
* Correspondence: sol14net@yahoo.com

Abstract: Microgrids of varying size and applications are regarded as a key feature of modernizing the power system. The protection of those systems, however, has become a major challenge and a popular research topic for the reason that it involves greater complexity than traditional distribution systems. This paper addresses the issue through a novel approach which utilizes detailed analysis of current and voltage waveforms through windowed fast Fourier and wavelet transforms. The fault detection scheme involves bagged decision trees which use input features extracted from the signal processing stage and selected by correlation analysis. The technique was tested on a microgrid model developed using PSCAD/EMTDS, which is inspired from an operational microgrid in Goldwind Sc. Tech. Co. Ltd, in Beijing, China. The results showed great level of effectiveness to accurately identify faults from other non-fault disturbances, precisely locate the fault and trigger opening of the right circuit breaker/s under different operation modes, fault resistances and other system disturbances.

Keywords: Microgrid; Protection; bagged decision tree; Wavelet; FFT

1. Introduction

Though there is little variation on the way microgrids are defined in literatures, microgrids can arguably be defined as groups of interconnected distributed energy resources (DERs) and loads at distribution level with a specified electrical boundary and functionality to operate both in parallel with the utility grid and in island. Deployment of microgrids is getting momentum in recent years. There are a range of factors contributing for growing acceptance of microgrid in different parts of the world. In areas without access for electricity from grid, microgrid is not an option but an irremissible. However, the need for microgrids is not limited to those geographically isolated areas only. The increased demand for power supply reliability and susceptibility of the large grids for blackouts and short term interruptions related to natural disasters or other lower magnitude technical and natural events has contributed to microgrid becoming a popular choice in the already electrified areas. There is a way of thinking getting more ground in recent days that the complex and bulky power grid shall rather be modified to an aggregation of smaller microgrids. Microgrids ensure higher reliability for the customers with the supply availability during grid outages as well as allow higher flexibility in the way to produce and utilize electricity.

As equal as the wide acceptance and interest in microgrids, there are few but critical technical challenges in practicing the technology. One of those critical challenges is their protection. Bidirectional current flow, varying fault current levels, continuous variations in system arrangement and mode of operation and largely fluctuating nature of renewable DERs contribute for the complexity of microgrid protection and the need for advanced techniques. This paper addresses this issue by recommending and testing an effective technique of detecting faults in a microgrid that can satisfy the required selectivity and reliability of a protection system.

The major challenges in protection of microgrids arise from the construction features of a microgrid which involve large scale presence of converter type DERs and the possibility of two way power flow. That is to be added to the low inertia of the systems especially during island mode of operation. This makes them easily susceptible for instability due to changes in load and generation. The issue of less stable generation is a more common phenomenon as it is customary for microgrids to be dominated by renewable sources which have intermittent nature. Such conditions make protection of microgrids a challenging task by causing:

- Varying magnitude of fault current based on mode of operation and changes in configuration
- Low fault current in island mode
- Multiple fault sources and bidirectional current flow

Overcurrent protection through utilization of simple overcurrent relays and/or fuses was a common practice in the traditional low voltage distribution system. However, such traditional current magnitude based protection has been proved to lack the effectiveness demanded in today's distribution systems involving distributed generation and microgrids [1, 2].

The challenges in protection of microgrids due to their special nature have attracted researchers and scientists to work on and suggest different strategies. Some of the recommended techniques include park transformation [3, 4], adding fault current source [3], Artificial Neural Network [4] and voltage restrained over-current relaying [3], magnitude and angle of the superimposed negative and positive sequence current [5] or impedance [1], harmonic distortion based methods [3] and techniques involving wavelet transform [4]. A detailed review on the different fault diagnosis tools in the literature in available in [6].

One of the techniques used in order to achieve the required level of reliability in protection of microgrids is using different type of signal analysis tools to transform the voltage or current signals to features which can be used to identify faults. Some of such transforms applied in microgrid protection studies are park (abc to dq0) transformation, Fourier transform (DFT and FFT), wavelet transform (WT) and Hilbert-Huang transform (HHT).

Reference [4] employed an approach incorporating abc to dq0 transformation of the three-phase current and filtering the dq0 components through the wavelet transformation to detect faults using the finite difference between samples of the filtered signal. It was reported that the procedure was effective to detect high impedance faults. Another study [7] proposed a two stage protection scheme where the type of the fault is identified by monitoring the drop in amplitude of the fundamental frequency component of the voltage signal and fault location is identified by calculating the total harmonics distortion (THD). The paper recommended the applicability of the protection scheme as a backup or complementary for the main protection devices referring to the potential malfunctioning in case of a network comprising several dynamic loads. Reference [8] used wavelet transformation with dq0 decomposition to extract the high frequency details for fault location and isolation. The use of park transform is claimed to be an effort to reduce the computation time. The fault detection and location are both done by comparing the calculated parameters with a pre-set threshold which would influence the performance of the scheme under variations in configuration. While another study on time-frequency-based differential scheme through S-transform by [9] reported that the method can reliably protect the microgrid against different faults, [10] argues that HHT based technique demonstrated an even better performance compared to that of S-transform.

Most of the studies applying signal processing tools examined the effectiveness of using the transforms individually or in comparison with each other. The option of utilizing the transforms in parallel and where they are effective is not covered well. The other gap in the literature is the trend to keep using a predefined threshold to judge the occurrence of faults. Though the use of the transforms is an advancement to the traditional magnitude-only based approaches, the use of pre-decided threshold values is not convenient for microgrids where the fault current and hence the transformed parameters would significantly vary based on configuration and weather condition in case of renewables. Using adaptive setting values is recommended in some literatures while the need for sophisticated communication and the delay in online calculation of setting values are the bottlenecks for such an approach.

One option which compromises between the use of a fixed pre-defined threshold and communication based adaptive settings is the one involving soft computing approaches where the judgment on fault occurrence is decided from past experience through somewhat a 'black box' model. Some of the soft computing approaches investigated in microgrid protection studies are deep neural networks [11], Support vector Machines (SVM) [12], Adaptive Neuro-Fuzzy inference system (ANFIS) [11 and 12], decision trees [13-16].

Decision tree based data-mining models are employed in [15] and [16]. Reference [16] used discrete Fourier transform to preprocess the faulted current and voltage signals while [15] used Wavelet transform for the same purpose. Both papers reported achieving effective protection of the microgrid against faulty situations through their respective schemes. Reference [13] used a protection scheme involving Hilbert Space-Based Power (HSBP) algorithm as a primary protection and THD as backup protection and then ANFIS based decision maker to decide circuit breaker action. There are some recent studies on applying soft computing techniques with wavelet and Fourier transform in protection of microgrids. The option of combining wavelet transform and decision tree methods was tested in [15]. They reported to get satisfying results in detecting and locating faults under variations in operating conditions by making use of decision tree trained using wavelet transform based features of the current signals. Reference [11] is one of the latest attempts to make use of Discrete Wavelet transform (DWT) and deep learning algorithm in the form of gated recurrent unit (GRU) to address protection of microgrids. The paper utilized the time frequency domain features of the branch currents extracted through DWT given as inputs for three deep Neural Networks. They stated that they validated the fault detection mechanism's performance in providing accurate and timely fault type, phase, and location information.

Most of the studies on microgrid protection revolve around DC microgrids though there is a limited number of studies on AC microgrids as well. There are gaps in the available studies targeting AC microgrids in terms of the signal processing as well as incorporating bagged decision tree algorithm. Though the use of soft computing techniques together with signal analysis tools is seen to greatly improve the accuracy in detection and identifying the fault in some of the studies such, they either luck the comprehensiveness in incorporating both voltage and current measurements or the signal processing tools such as WT and FFT. The methods solely depending on current measurements suffer from the possible current transformer saturation. Those involving only either of the WT and FFT signal processing tools would miss the feature of frequency or time resolution from either methods both of which are of great importance in fault detection. The single decision tree based fault detection techniques are limited in capacity to entertain a large number of input features. Most of the studies are also seen to recommend extremely theoretical schemes which are too far from the state-of-art of the industrial protection schemes. In this study improving the well-known differential, directional and over-current protection schemes through the signal processing tools and the use of bagged decision trees is investigated.

Operation under different conditions was investigated by applying small and large changes in the generation and the loads, all kinds of faults at each branch of the microgrid in both gird-connected and island modes of operation. Effectiveness of the suggested scheme for solid and high impedance faults is also examined by applying faults of different fault resistances. The devised approach was tested on a test microgrid consisting of multiple converter-type DERs modeled using PSCAD4.6. The model microgrid is inspired from an operational microgrid in Goldwind Sc. & Tech. Co. Ltd. in Beijing, China. Current and voltage waveforms are recorded and transferred to MATLAB R2017b environment for further analysis to make the judgments about the occurrence and location of fault. The protection scheme involves extracting the features for fault detection from the current and voltage records through windowed fast Fourier transform (WFFT) and windowed wavelet transform (WWT). The extracted features from WWT are the change in magnitude of the approximation (ΔEa) and detail components (ΔEdn) and the change in number of Peak values of Wavelet coefficients (ΔNp). Change in magnitude of individual harmonic components (ΔHn) and phase angle of the fundamental frequency component (Ang) are calculated from the WFFT analysis. After the most important features are selected from a candidate list of features through correlation analysis, bagged

Peer-reviewed version available at Electronics 2018, 7, 61; doi:10.3390/electronics7050061

decision trees are trained and tested for detecting faults at the different zones (components) of the test microgrid.

The devised protection scheme is tested and proved to achieve the intended target of sensitive and selective operation without compromising reliability of the system. It is able to accurately identify the different faults from each other and other abnormal operating conditions that shouldn't necessitate tripping of a circuit breaker. It was superior to the conventional over current, directional and differential protections due to its higher sensitivity and accuracy in detecting and locating the faults. It also has the edge over adaptive relaying as it makes use of local measurements and avoids the need for communication and delayed calculation to frequently modify the relay settings.

2. Materials and Methods

The methodology applied in this paper is summarized in Figure 1. The first task is modeling the microgrid to be studied using PSCAD/EMTDS environment. A microgrid system inspired from an actual microgrid in Goldwind Sc. Tec. Co. Ltd in Beijing, China is adopted. The architecture and system components are described in more detail in the next sections. Different sets of faults and other disturbances are applied to the system for training and testing. The branch currents and bus voltages are recorded in PSCAD and the data is transferred to MATLAB for the next step of the study where the fault detection analysis is performed. This required transferring the file from the COMTRADE format which PSCAD saved the recorded data to a MATLAB matrix file. The recorded voltage and current signals are first preprocessed using the two signal analysis tools, WT and FFT over a moving window with length of the period of the fundamental (0.02 Sec or 20 time steps based of 1000 us sampling step). Then after, the candidate features (ΔEa, ΔEdn, ΔNp, ΔHn and Ang) are calculated. The need for signal processing tools was further verified and the where to use which features was decided through a correlation analysis stage. In this stage, correlation of all candidate features with the target parameters (state of breaker) are computed. The selected most important features are then used as input to train the bagged decision trees for detecting faults in the different zones (components) of the test microgrid.

2.1. Simulation Model of Test Microgrid

A non-isolated microgrid model consisting of two converter based DERs and two loads connected in an arrangement as shown in the single line diagram in Figure 2 is developed using PSCAD/EMTDS software. The two DERs are solid-state converter based and the architecture of the converter topology employed in both sources is as shown in Figure 3. The presence of soli-state converters is a critical issue in the analysis of protection of microgrids for the reason that the current that can be supplied through such converter based DERs is mostly limited to a maximum of twice the rated current. This limits the fault current amount which intern causes sensitivity issues in protection of microgrids.

Each one of the system components are connected to their respective busbars through a circuit breaker and a current transformer represented as multi-meter. The system architecture and some of the components are made to resemble the actual and operational Goldwind microgrid in Beijing, China. The microgrid consists of four busbars and it is connected to the grid and hence has the capability to operate in both grid connected and island modes. Both modes of operation are evaluated in the study.

The two DERs operate in PQ mode generating the amount of power specified in Table 1 under reference normal operating case. The output active and reactive power from the DERs and the amount of power supplied to the load are varied in order to observe and record the respective changes in the current and voltage waveforms. The change in generation is implemented by varying the reference active and reactive powers in the converter control of the DERs. The PQ control circuit of the DERs' converters consist of two cascaded loops, namely an internal current loop and an external voltage loop. The control circuit is shown in Figure 4. Hysteresis band based technique is employed to generate the gate signals of the converter.

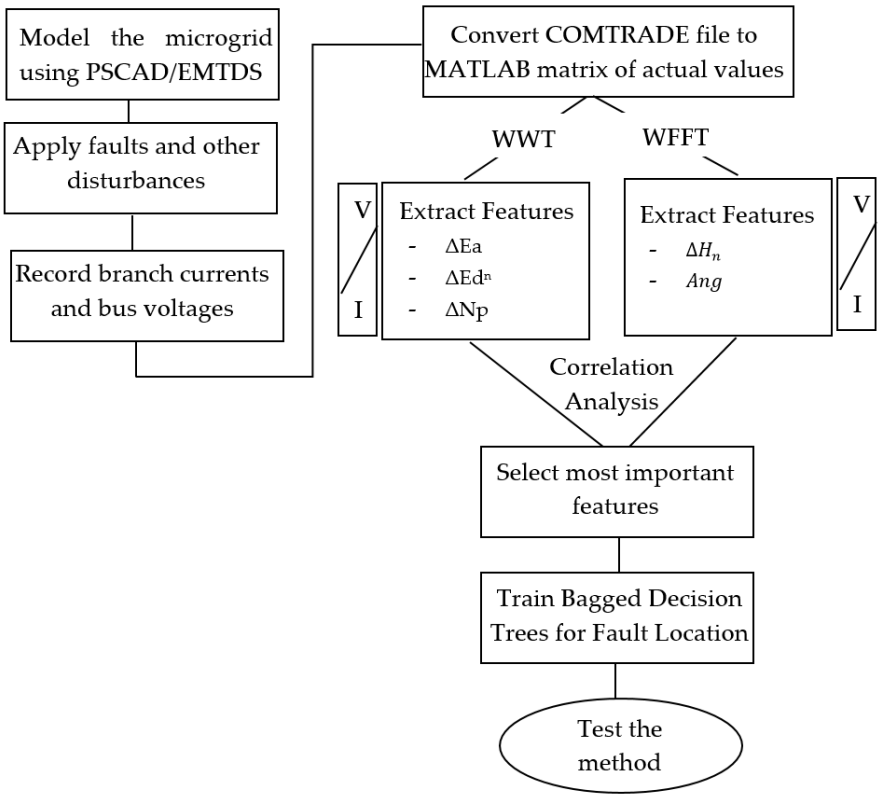

Figure 1. Summary of Methodology of the Study

Table 1. System components of Test Microgrid under reference normal operation

Component	Capacity (kW)	
	Grid-connected	Island
DER1	30	30
DER2	30	-
Load1	20	22
Load2	20	12
Grid	Inf.	-

While the microgrid operates in island mode, one of the DERs (DER2) will start operating in U/f mode serving as a voltage and frequency reference for the microgrid system taking the place of the grid in grid-connected mode. In this case the possible variation in generation is simulated by changes in the other DER (DER1). The control circuit used to control the voltage and frequency of the U/f mode DER is shown in Figure 5.

The following types of faults are applied and investigated on the protection zones showed in Figure 6.

- Single Line to Ground faults (LG)
- Line to Line faults (LL)
- Double Line to Ground faults (LLG)
- Three Phase to Ground faults (LLLG)

Both solid and high impedance faults (HIF) are studied.

Preprints (www.preprints.org) | NOT PEER-REVIEWED | Posted: 30 March 2018 doi:10.20944/preprints201803.0272.v1

Peer-reviewed version available at Electronics 2018, 7, 61; doi:10.3390/electronics7050061

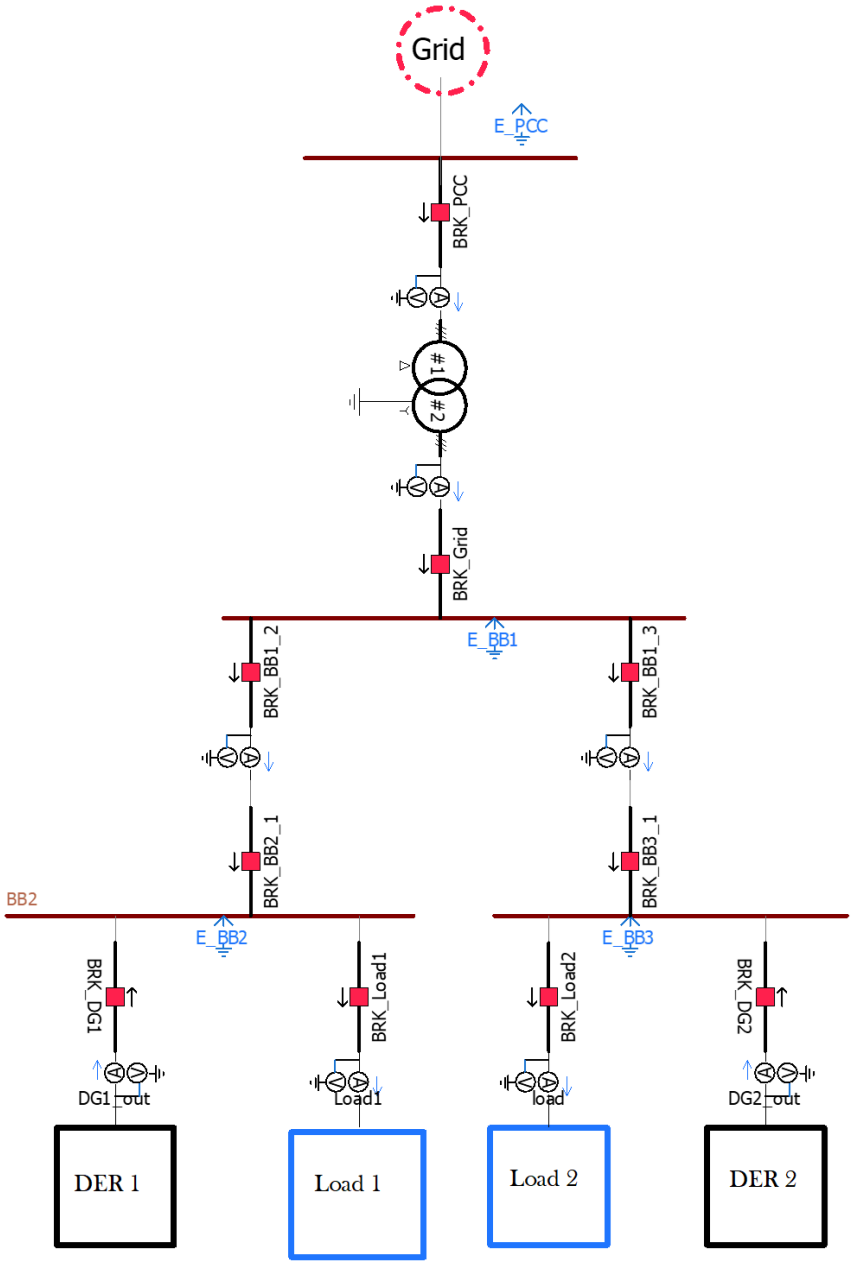

Figure 2. Microgrid test Model in PSCAD/EMTDS

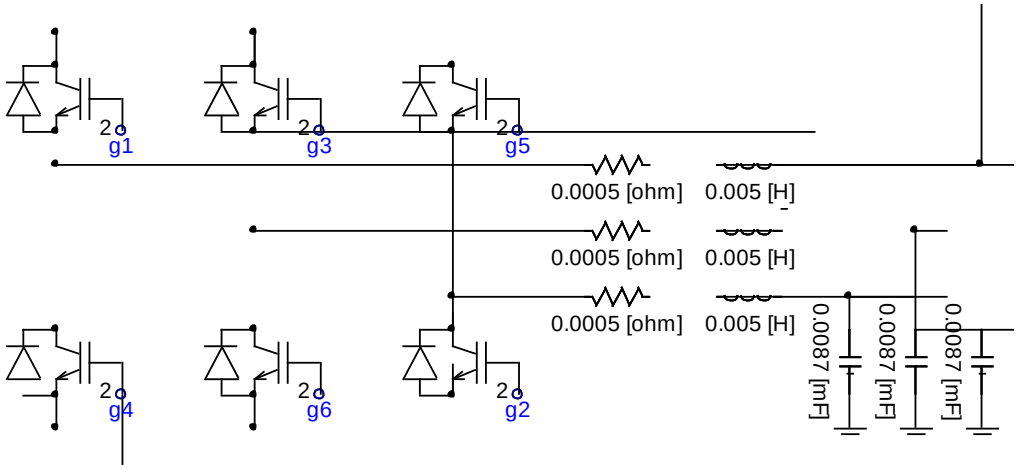

Figure 3. Converter topology of the DERs in the test microgrid

Preprints (www.preprints.org) | NOT PEER-REVIEWED | Posted: 30 March 2018 doi:10.20944/preprints201803.0272.v1

Peer-reviewed version available at Electronics 2018, 7, 61; doi:10.3390/electronics7050061

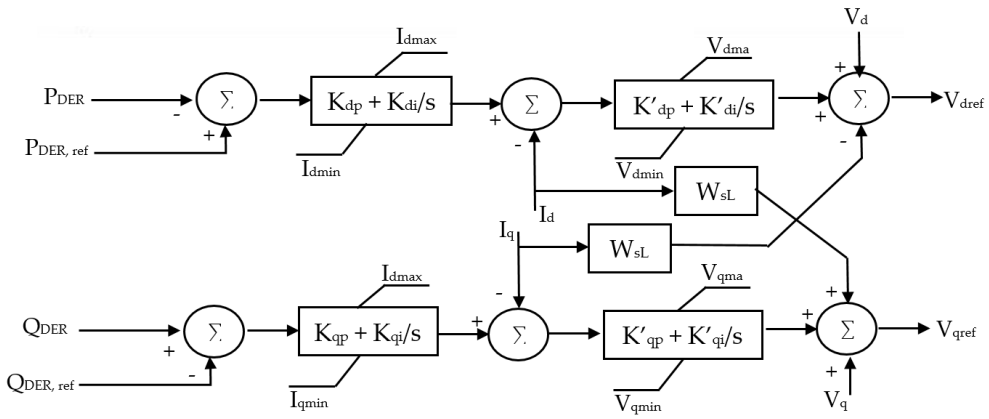

Figure 4. Control circuit block diagram of converters of the PQ controlled DERs

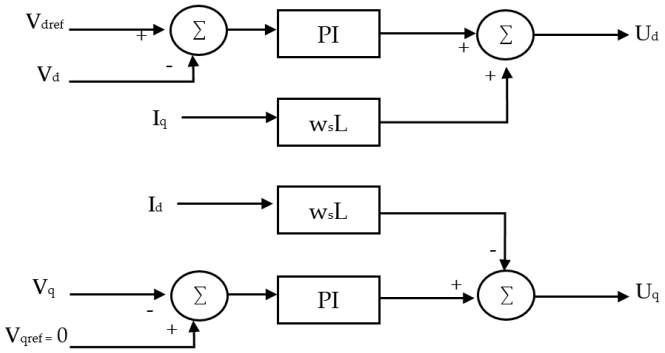

Figure 5. Control circuit block diagram of converters of the U/f controlled DER in island mode

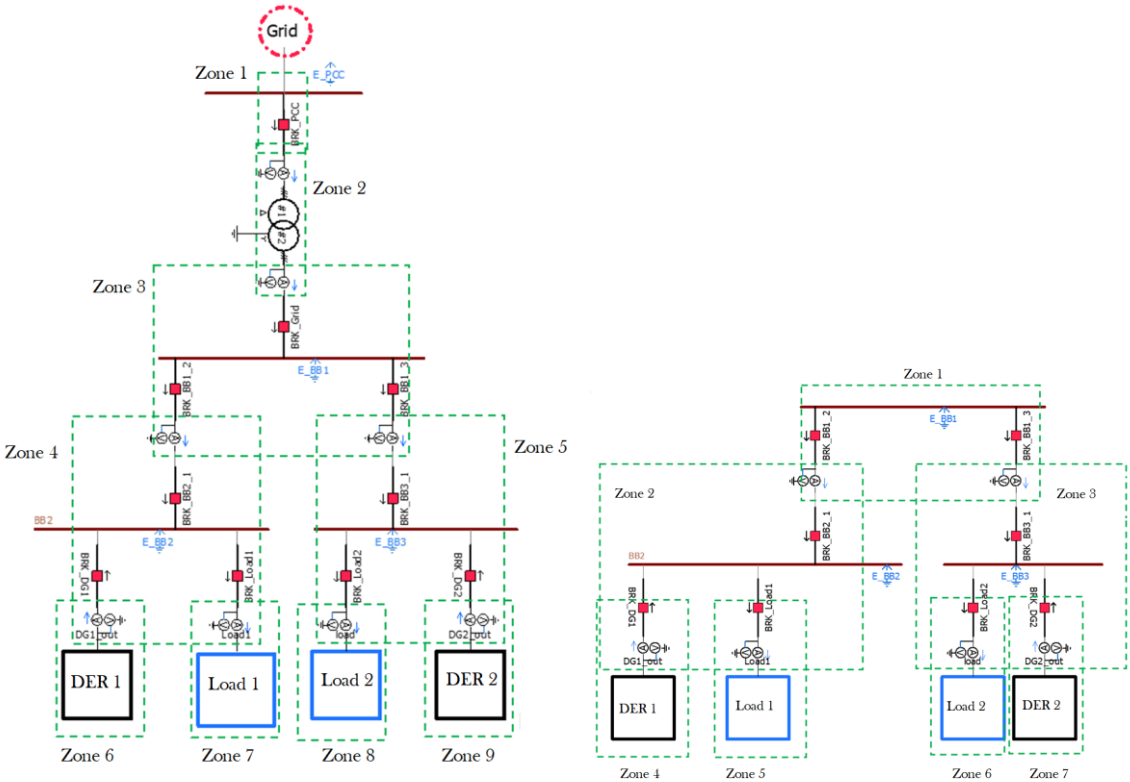

(a) **(b)**

Figure 6. Protection Zones for Fault Analysis in case of **(a)** grid-connected **(b)** island modes of operation

The study investigates the applicability of the suggested protection scheme to effectively identify faults from non-fault abnormal conditions. This involves training and testing a model based on recorded and transformed waveforms of the circuit reacting to the following sets of sadden changes in the system. The fault and disturbance cases shown in Table 2 are applied on the test microgrid model for training the bagged decision tree based fault detecting model. All the tests are conducted in both grid-connected and island modes of operation.

Table 2. Faults and disturbances for training

Type of Fault		LG, LL, LLG, LLLG (4)
Fault Location	-	At each bus bar (4^1, 3^2)
	-	At each component (2 DREs, 2 loads, 1 transformer) (5^1, 4^2)
	-	At each of the connection lines between buses (3^1, 2^2)
Fault Resistance (Ω)		0 (solid fault), 0.2 (HIF)
Sudden Change in generation	-	Additional 10 kW from DER1
	-	10kW Reduction in generation of from DER1
	-	Disconnect DER1
	-	Additional 15 kW from DER2 [1]
	-	15 kW Reduction in generation of from DER2 [1]
	-	Additional 15 kW from DER2 [1]
	-	Connect back DER1
Sudden Change in load	-	Addition of 20 kW [1] (15 kW [2]) to Load1
	-	Removal of 20 kW from Load1
	-	Addition of 10kW to Load2
	-	Removal of 10 kW from Load2
	-	Disconnect Load1
	-	Connect back Load1

[1] for grid connected only, [2] for island mode only

Table 3 shows the different fault and disturbance cases applied on the test microgrid model to test and evaluate the performance of the devised protection scheme.

Table 3. Faults and disturbances for testing

Type of Fault		LG, LL, LLG, LLLG (4)
Fault Location	-	At a selected bus bar (1)
	-	At one DER and one load (2)
Fault Resistance (Ω)		0 (solid fault), 0.1, 0.125, 0.15, 0.2
Sudden Change in generation	-	Additional 10 kW from DER1
	-	10kW Reduction in generation of from DER1
	-	Additional 15 kW from DER2 [1]
	-	15 kW Reduction in generation of from DER2 [1]
	-	Additional 15 kW from DER2 [1]
	-	Disconnect DER2
	-	Connect back DER2
Sudden Change in load	-	Addition of 20 kW [1] (15 kW [2]) to Load1
	-	Removal of 20 kW from Load1
	-	Addition of 10kW to Load2
	-	Removal of 10 kW from Load2
	-	Disconnect Load2
	-	Connect back Load2

[1] for grid connected only, [2] for island mode only

Preprints (www.preprints.org) | NOT PEER-REVIEWED | Posted: 30 March 2018 doi:10.20944/preprints201803.0272.v1

Peer-reviewed version available at Electronics 2018, 7, 61; doi:10.3390/electronics7050061

2.2. Signal Analysis and Features

2.2.1. Windowed Fast Fourier Transform and Derived Features

Fourier transform is a very popular technique in analysis of signals, especially those of which are periodic. It, essentially, breaks down a signal into a combination of sine waves of different amplitudes and frequencies as mathematically expressed in Equation (1).

$$F(jw)=\int_{-\infty}^{+\infty} f(t)e^{-jwt}dt \qquad \text{or} \qquad f(t)=\frac{1}{2\pi}\int_{-\infty}^{+\infty} F(jw)e^{jwt}dw \tag{1}$$

This and similar studies in fault analysis involve discrete waveforms which are recorded voltage and/or current signals of specified sampling interval. In such cases the type of Fourier transform to be applied will be discrete Fourier transform (DFT). DFT of a signal such as current waveform in our case is defined by equation (2). Fast Fourier transform (FFT) is optimized implementation of a DFT

$$X(w^{jw})=\sum_{n=-\infty}^{+\infty} x[n]e^{-jwn} \qquad \text{or} \qquad x[n]=\frac{1}{2\pi}\int X(e^{jw})e^{jwn}dw \tag{2}$$

with less computation but essentially the same principle as DFT. The central point behind the computation time requirements in DFT and FFT lies in the fact that DFT involves N^2 arithmetic operations, while FFT needs only $N\ log(N)$. This is achieved by converting discrete Fourier transform of a sequence of N points into two discrete Fourier transforms of length N/2 each. Equation (3) expresses how this is done in FFT.

$$X[k]=\sum_{n=0}^{N-1} x[n]W_N^{nk}=\sum_{\substack{n=0\\ \text{even n}}}^{N-1} x[n]W_N^{nk}+\sum_{\substack{n=0\\ \text{odd n}}}^{N-1} x[n]W_N^{nk} \tag{3}$$

Fourier transform has a major drawback in its failure to provide information about the timing of change in frequencies or magnitude. The time aspect of a signal is as important or even more important feature in fault analysis studies. Hence we have options of using a windowed form of the Fourier transform to cover up for this gap in Fourier transform. Windowed Fourier Transform is a form of Fourier transform in which the sinusoidal wave of the Fourier transform is replaced by the product of a sinusoid and a window which is localized in time. This enable to capture not only the frequency information but the time information of the signal as well. Windowed FFT is thus nothing but equivalent to a sequence of FFTs. It can be mathematically expressed as:

$$Sf[m.l]=\langle f,g_{m.l}\rangle \tag{4}$$

$$=\sum_{n=0}^{N-1} f[n]g[n-m]e^{\frac{-j2\pi ln}{N}} \tag{5}$$

where g is the windowing function, and the computation is performed with N FFTs.

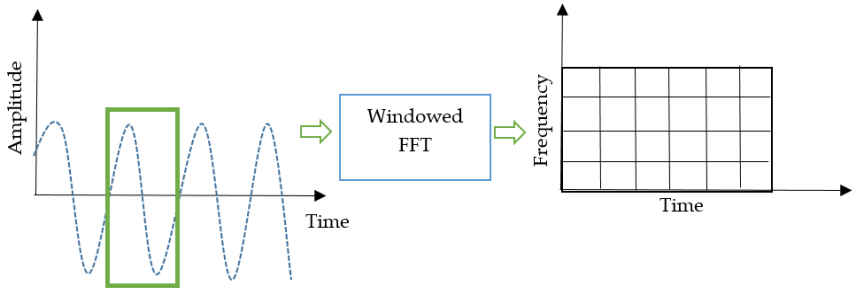

Figure 7. Windowed FFT

Preprints (www.preprints.org) | NOT PEER-REVIEWED | Posted: 30 March 2018 doi:10.20944/preprints201803.0272.v1

Peer-reviewed version available at Electronics 2018, 7, 61; doi:10.3390/electronics7050061

Features of the voltage and current signals derived from the winnowed Fourier transform are used in this study to evaluate the occurrence of a fault. These features are the change in magnitudes of individual harmonic components of voltage and current waveforms and phase angles of the first harmonics (the fundamental component). Magnitude of n^{th} harmonic $\boldsymbol{H_n(i)}$ and angle of the first harmonics $\boldsymbol{Ang(i)}$ in the i^{th} window are extracted from the FFT analysis as shown in Equations (6) and (7).

$$H_n(i)=|V^n(i)| \tag{6}$$

$$Ang(i)=angle(V^1(i)) \tag{7}$$

The change in magnitude of n^{th} harmonic in the i^{th} window is calculated by subtracting the average of the magnitudes of the harmonics in the previous cycle to the magnitude of the harmonic in the i^{th} window.

$$\Delta \boldsymbol{H_n(i)} = \boldsymbol{H_n(i)} - \frac{\sum_{j=i-N}^{i-1} \boldsymbol{H_n(j)}}{\boldsymbol{N}} \tag{8}$$

Where N is the number of samples in a cycle, which is 20 in our case based on a recording time step of 1 ms.

The n^{th} level harmonic component of the voltage signal samples in the i^{th} window of transformation ($V^n(i)$) can thus be expressed as:

$$V^n(i)=H_n(i)e^{Ang(i)} \tag{9}$$

2.2.2. Windowed Wavelet Transform and Derived Features

Wavelet transform is a comparatively recent tool of signal analysis targeted at addressing limitations in Fourier transform by filling in the limited time resolution capability in Fourier transform. This enables the transform to keep information of both time and frequency in the signal. It is an ideal tool particularly for analysis of non-stationary signals such as fault current/voltage signals where the sudden changes in signal pattern is studied to detect and locate faults. Wavelet transform decomposes a signal into a combination of multiples of scaled and shifted mother wavelet resulting in the so-called "Approximation" and "Detail" components. The approximation component is a high-scale, low frequency component while the detail components represent those with low scale and high frequency. The two will appear as a pair in every stage of decomposition in the way as Figure 8.

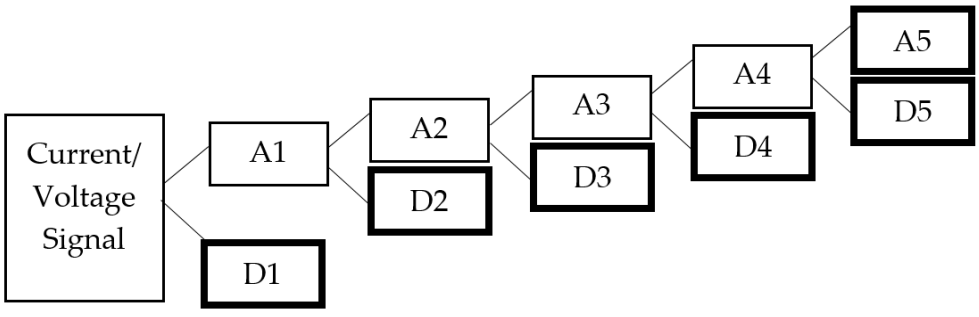

Figure 8. Wavelet Decomposition of Current/ Voltage Signals

The single level wavelet decomposition of a voltage signal V[i], which is sampled data of the continuous voltage signal V(t), can be mathematically expressed as:

Preprints (www.preprints.org) | NOT PEER-REVIEWED | Posted: 30 March 2018 doi:10.20944/preprints201803.0272.v1

Peer-reviewed version available at Electronics 2018, 7, 61; doi:10.3390/electronics7050061

$$y[i]=(V*g)[i]=\sum_{k=-\infty}^{\infty} V[k]g[i-k] \quad (10)$$

where g represents the impulse response of the low pass filter.

Outputs of the low and high pass filters which are usually called approximation and detail components are also expressed by (12) and (13).

$$V_{low}[n]=\sum_{i=-\infty}^{\infty} V[k]g[2n-i] \quad (12)$$

$$V_{high}[n]=\sum_{i=-\infty}^{\infty} V[k]h[2n-i] \quad (13)$$

where h is the high pass filet transfer function.

The integral part of wavelet Analysis is the mother wavelet. The mother wavelet is an equivalent of the sinusoid in Fourier analysis. Nevertheless, it significantly differs from sinusoid in having a definite end and varying shape unlike a sinusoid. The choice of the mother wavelet from available families such as Mexican Hat, Haar, Daubechies, Coiflets, Morlet, etc. is one of the decisions to make in wavelet analysis. After a thorough try-and-errors and review of related literatures, 'haar' wavelet is selected for this study. The selection is made based on how the features resulted from the wavelet transform can help to identify faults from non-fault conditions.

The change in Wavelet energy of the approximation (ΔEa) and detail components (ΔEd^n) and change in number of Peak values of Wavelet coefficients (ΔNp) are the two features used in this study based on wavelet transform of the voltage and current signals. Wavelet energy is the percentage of energy corresponding to the approximation and the details.

$$Ea(i)=\sum_{j=1}^{N} |A_{ij}|^2 \quad (14)$$

$$Ed^n(i)=\sum_{j=1}^{N} |D^n_{ij}|^2 \quad (15)$$

where A_{ij} is the j^{th} element in the approximation coefficient matrix of the i^{th} window and $D^n{}_{ij}$ is the j^{th} element in the n^{th} level detail coefficient matrix of the i^{th} window

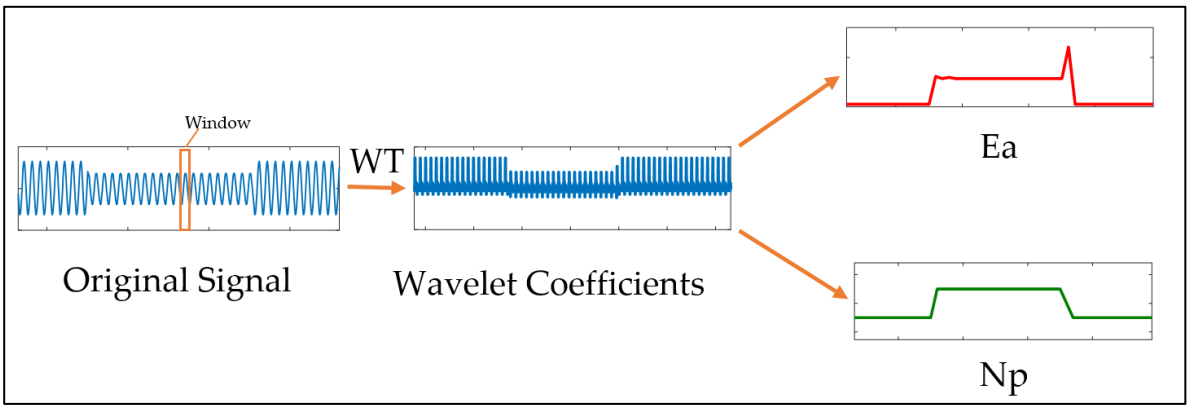

Figure 9. Wavelet transform over a moving window and Features

The changes in approximate and detail wavelet energies are then calculated as in Equation (16) and (17).

$$\Delta Ea(i)= Ea(i)-\frac{\sum_{j=i-N}^{i-1} Ea(j)}{N} \quad (16)$$

Preprints (www.preprints.org) | NOT PEER-REVIEWED | Posted: 30 March 2018 doi:10.20944/preprints201803.0272.v1

Peer-reviewed version available at Electronics 2018, 7, 61; doi:10.3390/electronics7050061

$$\Delta Ed^n(i) = Ed^n(i) - \frac{\sum_{j=i-N}^{i-1} Ed^n(j)}{N} \quad (17)$$

The other feature extracted from the windowed WT is change in number of Peak values of Wavelet coefficients (ΔNp). The use of number of peak values of Wavelet coefficients is adopted from [17] though the parameter is applied specifically for power quality assessment rather than protection study in the paper. If Np(i) is the number of peak values in the i^{th} window, the change in number of peaks ΔNp(i) can be calculated as the difference between Np(i) and average of the last cycle.

$$\Delta N_p = N_p(i) - \frac{\sum_{j=i-N}^{i-1} N_p(j)}{N} \quad (18)$$

2.2.3. Correlation Analysis for Feature Selection

The inputs for the fault detection module based on bagged decision trees is decided through a set of correlation analysis at each zone of protection or protected component. The correlation analysis evaluates the relative importance of the candidate features to the decision of existence of fault by measuring the strength and direction of the linear relationship between two variables: the selected features and intended state of the concerned circuit breaker.

$$Corr(X,Y) = \frac{\sum_m \sum_n (X_{mn} - \bar{X})(Y_{mn} - \bar{Y})}{\sum_m \sum_n (X_{mn} - \bar{X})^2 (Y_{mn} - \bar{Y})^2} \quad (19)$$

where $\bar{X}$ = *mean(X),* and $\bar{Y}$ = *mean(Y)*

2.3 Bagged Decision Trees

Decision trees are one of the data mining techniques that has been used for classification applications for a number of years [18]. The method has seen recent revival due to higher accuracy being achieved through the discovery of methods of ensembling of more than one trees [19, 20].

A decision tree is a technique where complex problems are broken down into a hierarchy of simpler ones. A hierarchical structure of connected nodes forms a decision tree as it can be seen in Figure 10. While training a decision tree, all training data is sent into the tree in order to optimize the parameters of the internal nodes. Testing of a decision tree involves repeated binary testing of an input data at internal nodes and the result being sent to the appropriate (the right or left) child until it reaches a terminal node (leaf). The leaf nodes usually contain a predictor (a classifier in this case) that will associates an output (a class label of 1 or 0 to represent existence or non-existence of a fault) to the input features.

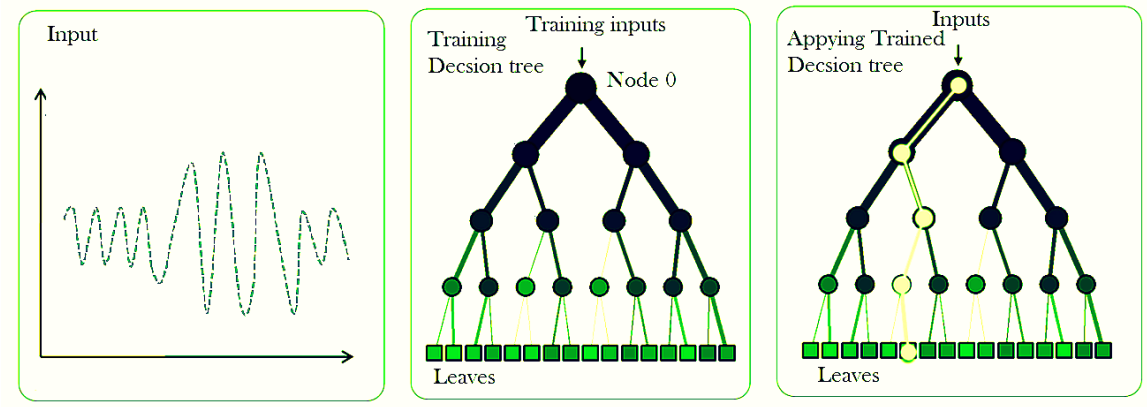

Figure 10. Training and Applying decision trees

Making the decision on training optimal number of decision trees has been a long standing problem and it has recently emerged that using an ensemble of learners would yield greater accuracy

Preprints (www.preprints.org) | NOT PEER-REVIEWED | Posted: 30 March 2018 doi:10.20944/preprints201803.0272.v1

Peer-reviewed version available at Electronics 2018, 7, 61; doi:10.3390/electronics7050061

and generalization. One of the attempts is an iterative re-weighting of training data to build more accurate classifiers which is a boosting algorithm by [21].

Bootstrap-aggregated (bagged) decision trees that combine the results of many decision trees address the issue of individual decision trees tendency to overfit. This approach reduces the effects of overfitting and improves generalization, and is the method adopted in this study. Bagged decision trees use an ensemble of decision trees using a bootstrap samples of the data. The technique resembles random forest algorithm in the fact that it selects a random subset of predictors to use at each decision split. In case of oversampling classes decision with large misclassification, the bagged costs tree generates in-bag samples while it generates undersampling classes for small misclassification costs.

Bagged decision trees has become the choice of this paper due to their effectiveness in mapping more than one input parameters to a target classification variable, which in our case is the state of the circuit breaker. An individual set of bagged decision trees is trained and applied for each zone of protection and each phase with different sets of inputs based on the result of the correlation analysis. As it can be seen in Figure 11, at each node the selected input features are compared with threshold values updated by the training stage and decision are made to pass to the right or left node in the next hierarchy. This ends with the last node (leaf) where the binary decision on the state of the circuit breaker is made.

Table 4. Description of the bagged decision tree employed in this study

Parameter	Value
Method	classification
Number of variables to select at random for each decision split	All / 1 – based on try and error
Numeric vector of prior probabilities for each class.	Empirical
Optimizer	Bayesian optimization

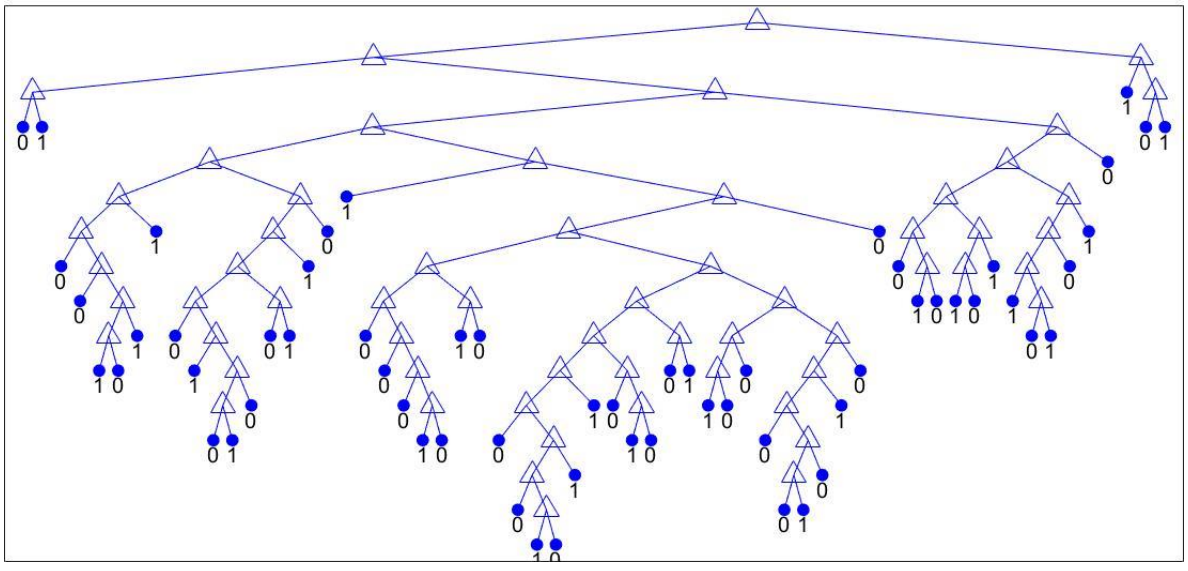

Figure 11. Graphical View of bagged decision trees

3. Results and Discussions

3.1. Grid-connected Mode

In this section, the results from correlation analysis of the candidate features and testing of the recommended method on a microgrid model operating under grid-connected mode are presented and discussed. The following sets of tests are done in the grid-connected mode:

1. Faults in Zone 1 (PCC bus Protection)

Preprints (www.preprints.org) | NOT PEER-REVIEWED | Posted: 30 March 2018 doi:10.20944/preprints201803.0272.v1

Peer-reviewed version available at Electronics 2018, 7, 61; doi:10.3390/electronics7050061

2. Faults in Zone 4 (Busbar protection)
3. Faults in Zone 6 (DER protection)
4. Faults in Zone 8 (Load protection)

3.1.1. Faults in Zone 1 (PCC bus Protection)

36 candidate features are tested for detecting fault in the PCC area. The correlation analysis results (shown in Table 5) are referred to select the most important features to use as input for the bagged decision trees. Out of the candidate features, 13 of them whose correlation is above 0.1 are selected.

Table 5. Selection of most important features for Zone 1 (PCC) protection

Rank	Corr	|Corr|	Parameter
1	0.274	0.274	ΔEa_VPCCA
2	-0.259	0.259	ΔNp_VPCCA
3	-0.225	0.225	ΔH_VPCCA(1)
4	-0.197	0.197	ΔEd_VPCCA(3)
5	-0.168	0.168	ΔEd_VPCCA(5)
6	-0.153	0.153	ΔEd_VPCCA(2)
7	0.153	0.153	ΔH_I1A(2)
8	0.146	0.146	ΔH_VPCCA(2)
9	0.144	0.144	ΔEd_I1A(3)
10	0.128	0.128	ΔH_I1A(4)
11	0.125	0.125	ΔH_I1A(5)
12	0.125	0.125	ΔH_I1A(7)
13	0.122	0.122	ΔH_I1A(10)

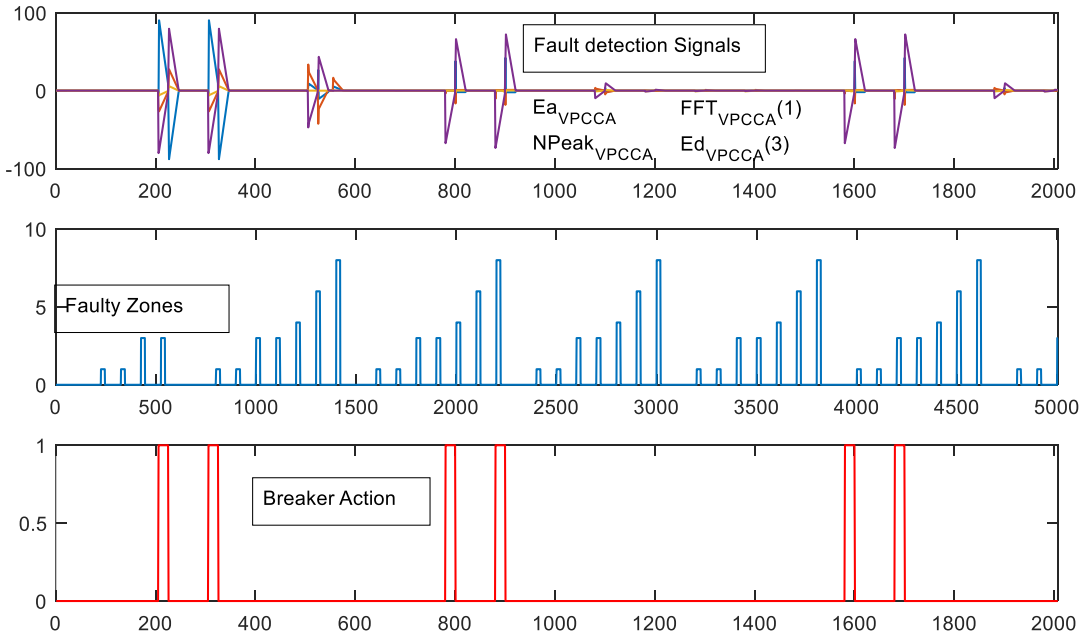

Figure 12. Fault detection signals and breaker action for a sequence of faults in Zone 1

Figure 12 shows four of the selected features versus the faulty zone and the respective breaker action. Not all inputs are displayed in the graph so as to avoid overcrowding in the display. As it can be seen from the figure, the selected features changed noticeably to effectively identify the fault conditions from normal operation and non-fault disturbances. Though faults were also applied on the other regions of the microgrid during the same period, the method was able to accurately identify

Preprints (www.preprints.org) | NOT PEER-REVIEWED | Posted: 30 March 2018 doi:10.20944/preprints201803.0272.v1

Peer-reviewed version available at Electronics 2018, 7, 61; doi:10.3390/electronics7050061

the location of the fault and hence trigger breaker action only during the fault in the concerned region. The summary of the method in the test case is further explained in Table.

Table 6. Performance and Confusion of the Fault Detection Method for faults in Zone 1

Parameter	Undetected	False detection
No of confusion	1001	41
Number of fault/ no fault points	11368	194712
Percentage Error (%)	8.8	0.02
Accuracy (%)	91.2	99.98

The method was effective to locate the fault with an accuracy of 92.1% with 1001 points out of the total 11,368 faulty points correctly identified. The method did exceptionally well in terms of avoiding false detection of non-fault conditions with a bare 0.02% error in that regard.

Though performance of the method is very good in terms of fault detection, the method showed little limitation in terms of considerable number of fault conditions passing unnoticed. This is, in one way, related to the high impedance faults under which the model performance is comparatively lower that the solid faults. The comparison of performance of the method under different types of faults including solid faults and high impedance faults is shown in Figure 13. The other factor is the magnitude of the fault current under grid-connected case being extremely high making the task of selecting a perfect threshold to discriminate faults of different zones a little bit difficult and tricky one. The fact that a fault is not detected to belong to this specific zone does not actually mean the method fails to detect such fault at all. Applying the same method to detect the occurrence of a fault in any of the zones in the microgrid showed an extremely high level of accuracy with 99.98% accuracy. So, the limitation was rather on locating the faults.

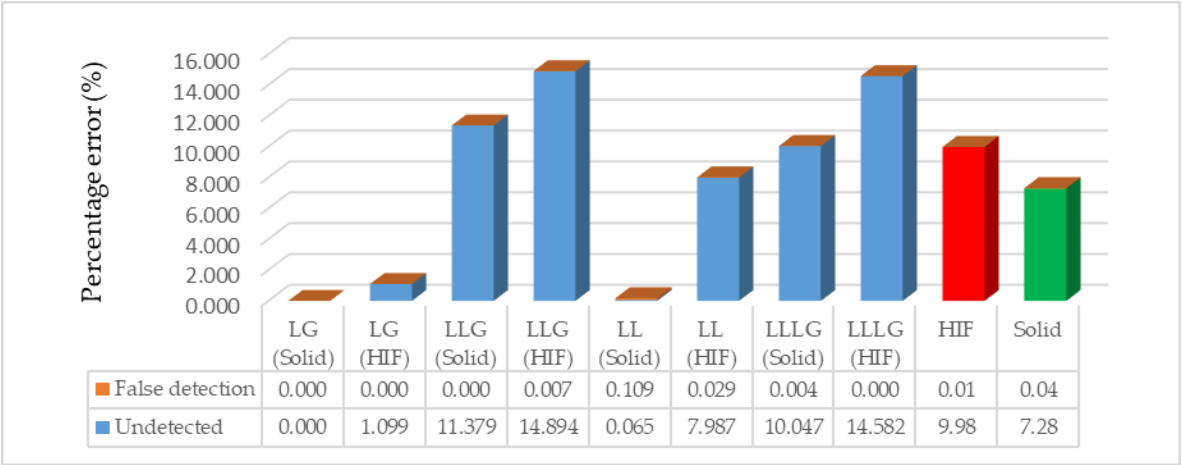

Figure 13. Comparison of performance of the Method for different types of faults in Zone 1

3.1.2. Fault in Zone 4 (Busbar protection)

The method was then tested for a sequence of faults of different type and resistance in Zone 4, which is one of the busbars in the microgrid. The method is compared to the conventional differential protection which is the most common method of protection for busbars. An additional input parameter, the root mean square (RMS) value of the differential current, is considered in this case. It is the most correlated feature as it might easily be expected while the other important features are those shown in Table 7.

Table 7. Selection of most important features for Zone 4 (Busbar 2) protection

Rank	Corr	|Corr|	Parameter

Preprints (www.preprints.org) | NOT PEER-REVIEWED | Posted: 30 March 2018 doi:10.20944/preprints201803.0272.v1

Peer-reviewed version available at Electronics 2018, 7, 61; doi:10.3390/electronics7050061

1	0.652	0.652	Idiff_BB2_RMS
2	0.120	0.120	ΔEa_VBB2A
3	-0.118	0.118	ΔNp_VBB2A
4	-0.118	0.118	ΔH_VBB2A(1)

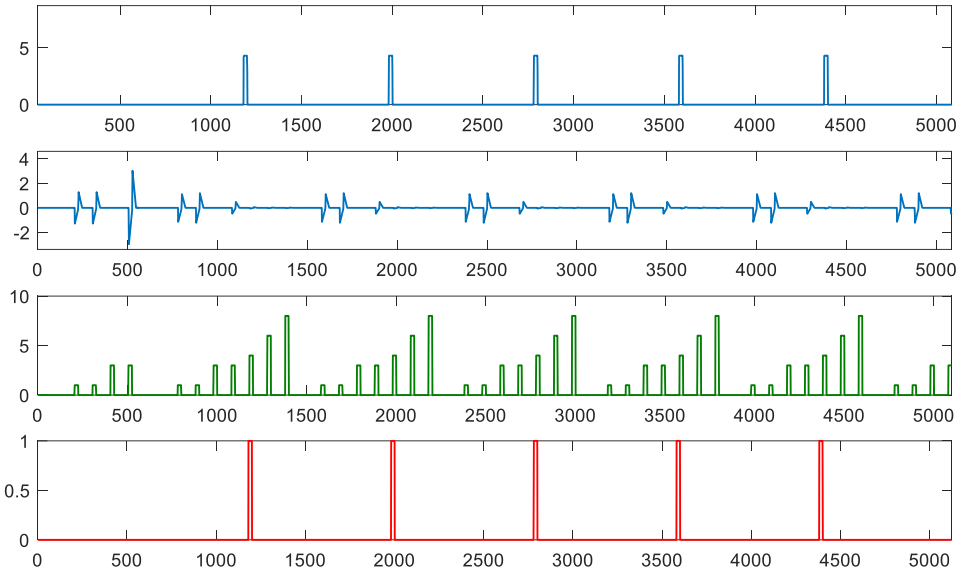

Figure 14. Fault detection signals and breaker action for a sequence of faults in Zone 4

Table 8. Performance of the Devised Method for different types of faults in Zone 4 (Busbar 2)

Type of Fault	Undetected			False detection		
	No. of points	Percentage Error (%)	Accuracy (%)	No. of points	Percentage Error (%)	Accuracy (%)
LG (Solid)	0	0.00	100.00	0	0.00	100.00
LG (HIF)	36	5.00	95.00	0	0.00	100.00
LLG (Solid)	36	5.00	95.00	0	0.00	100.00
LLG (HIF)	71	9.40	90.60	1	0.00	100.00
LL (Solid)	70	9.52	90.48	0	0.00	100.00
LL (HIF)	36	5.00	95.00	0	0.00	100.00
LLLG (Solid)	36	5.00	95.00	0	0.00	100.00
LLLG (HIF)	36	5.00	95.00	36	0.13	99.87
HIF	179	6.14	93.86	37	0.03	99.97

Performance of the method recommended in this study is compared with a conventional differential protection of 10% differential relay setting, i.e., the restraint current fixed to be 10% above the maximum operating current. The result is presented in Table 8.

Table 9. Performance of the devised fault detection Method and conventional differential protection for protection of Zone 4 (Busbar 2)

Parameter	Undetected		False detection	
	Devised Approach	Conventional Differential protection	Devised Approach	Conventional Differential protection
No of confusion	322	1619	37	179

Preprints (www.preprints.org) | NOT PEER-REVIEWED | Posted: 30 March 2018 doi:10.20944/preprints201803.0272.v1

Peer-reviewed version available at Electronics 2018, 7, 61; doi:10.3390/electronics7050061

Number of fault/ no fault points	5091	5091	200989	200989
Percentage Error (%)	6.32	31.80	0.02	0.09
Accuracy (%)	93.68	68.2	99.98	99.91

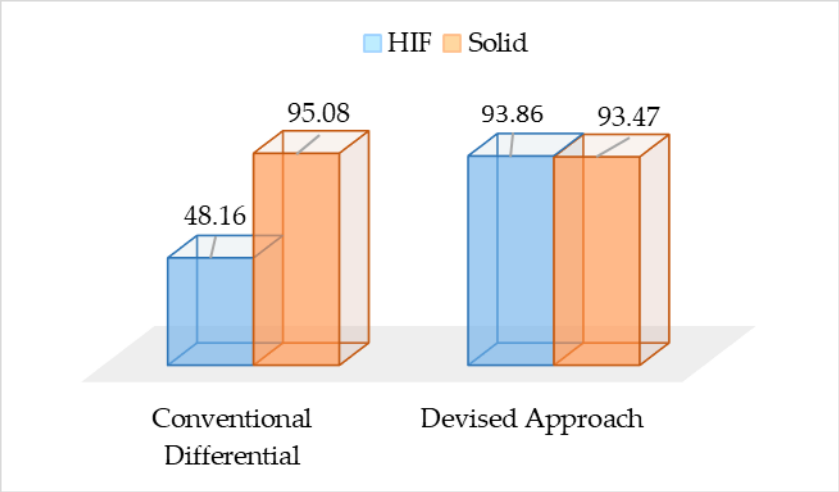

Figure 15. Comparison of devised approach against conventional differential protection for solid and high impedance faults

The devised approach showed greater level of selectivity compared to the most common protection for busbars, differential protection. The improvement is quit visible in case of HIFs with a performance as high as 93.86% compared to 45.08% of the conventional differential protection. The devised method's performance is seen to be slightly inferior in case of solid faults though.

3.1.3. Fault in Zone 6 (DER protection)

Distributed energy resources are the power suppliers in the microgrid. With the exception of energy storage systems, the current flow is expected to be in a specified direction. Hence, in case of protecting a DER, change in the direction of flow of current (and therefore the phase angle) would be a customary fault detection signal. That is where the addition of phase angle as an input features is assumed to play a great role. The correlation analysis result proved the same fact. As it can be seen from Table 10, the change in phase angle is one of the most important features together with other features extracted from the windowed FFT and WT analysis shown in Table 10.

Table 10. Selection of most important features for Zone 6 (DER) protection

Rank	Corr	|Corr|	parameter
1	0.413	0.413	ΔH_I5A(1)
2	0.223	0.223	Ang_I5A
3	0.122	0.122	ΔEa_VBB2A
4	-0.118	0.118	ΔNp_VBB2A
5	-0.116	0.116	ΔH_VBB2A(1)
6	-0.101	0.101	ΔH_I5A(3)

Preprints (www.preprints.org) | NOT PEER-REVIEWED | Posted: 30 March 2018 doi:10.20944/preprints201803.0272.v1

Peer-reviewed version available at Electronics 2018, 7, 61; doi:10.3390/electronics7050061

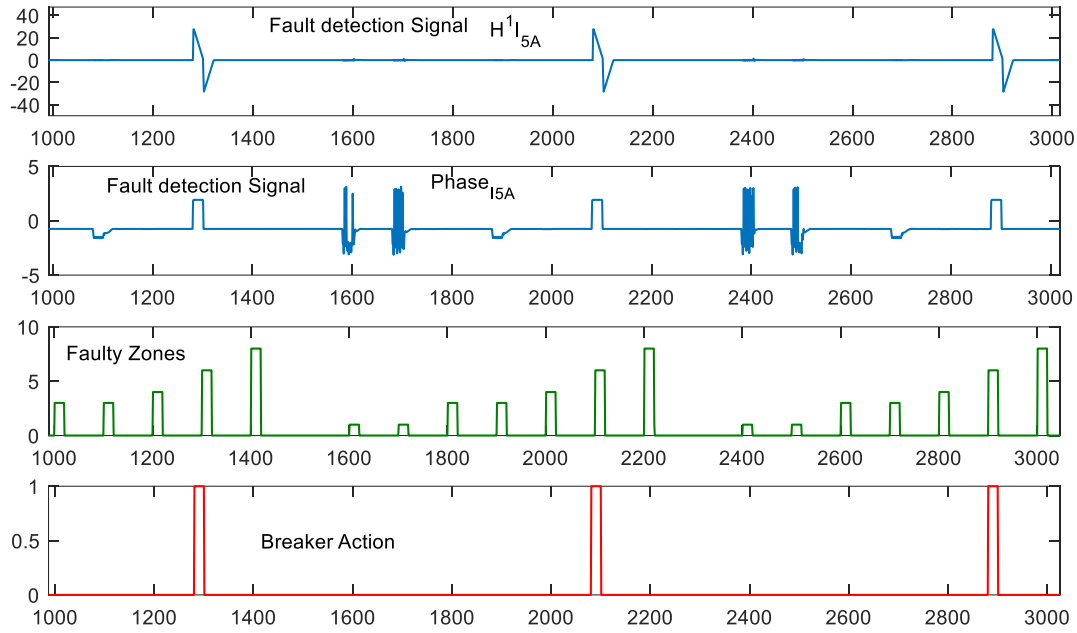

Figure 16. Fault detection signals and breaker action for a sequence of faults in Zone 6

Table 11. Performance of the Devised Method for different types of faults in Zone 6 (DER 1)

Type of Fault	Undetected			False detection		
	No. of points	Percentage Error (%)	Accuracy (%)	No. of points	Percentage Error (%)	Accuracy (%)
LG (Solid)	0	0.00	100.00	0	0.00	100.00
LG (HIF)	36	5.00	95.00	0	0.00	100.00
LLG (Solid)	35	4.86	95.14	0	0.00	100.00
LLG (HIF)	0	0.00	100.00	1	0.00	100.00
LL (Solid)	33	4.71	95.29	1	0.00	100.00
LL (HIF)	36	5.00	95.00	4	0.01	99.99
LLLG (Solid)	0	0.00	100.00	0	0.00	100.00
LLLG (HIF)	0	0.00	100.00	0	0.00	100.00
HIF	72	2.56	97.44	5	0.00	100.00
Solid	68	3.23	96.77	1	0.00	100.00
Total	140	2.85	97.15	6	0.00	100.00

The fault detection algorithm recommended in this study performed exceptionally well with faults in distributed energy resources. Almost no (only 6 points) false detection was exhibited from a total possibility of 201,028 points while the performance in accurately detecting test faults was also very high (97.15%). The method is farther compared with the option of using phase angle as the only fault detection signal to represent a simpler directional relay and the comparison is shown in Figure 17.

Preprints (www.preprints.org) | NOT PEER-REVIEWED | Posted: 30 March 2018 doi:10.20944/preprints201803.0272.v1

Peer-reviewed version available at Electronics 2018, 7, 61; doi:10.3390/electronics7050061

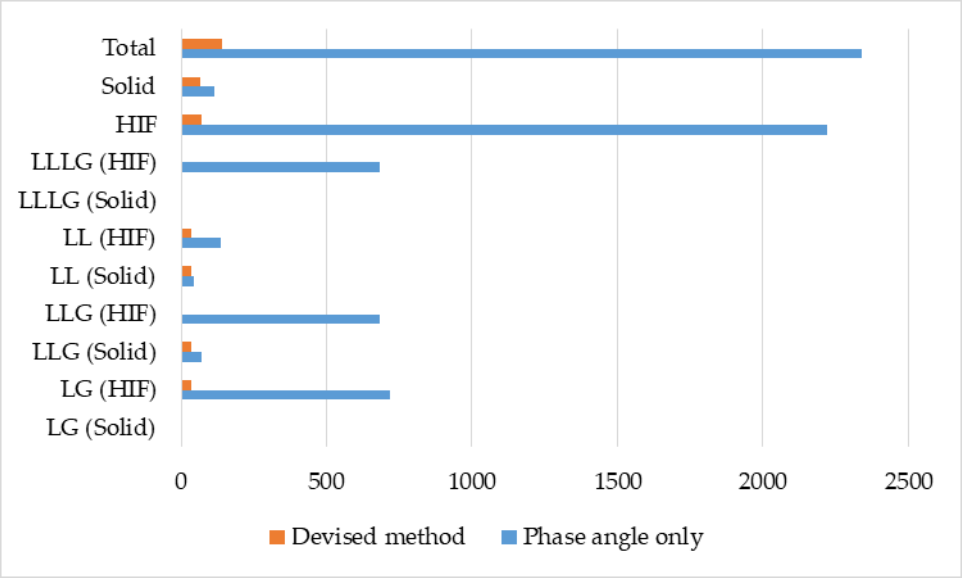

Figure 17. Comparing the option of using phase angle only with the devised approach

3.1.4. Fault in Zone 8 (Load Protection)

Table 12. Selection of most important features for Zone 8 (Load) protection

Rank	Corr	|Corr|	Parameter
1	0.418	0.418	ΔH_I8A(1)
2	0.124	0.124	ΔEa_VBB3A
3	-0.118	0.118	ΔNp_VBB3A
4	-0.114	0.114	ΔH_VBB3A(1)
5	-0.102	0.102	ΔH_I8A(3)

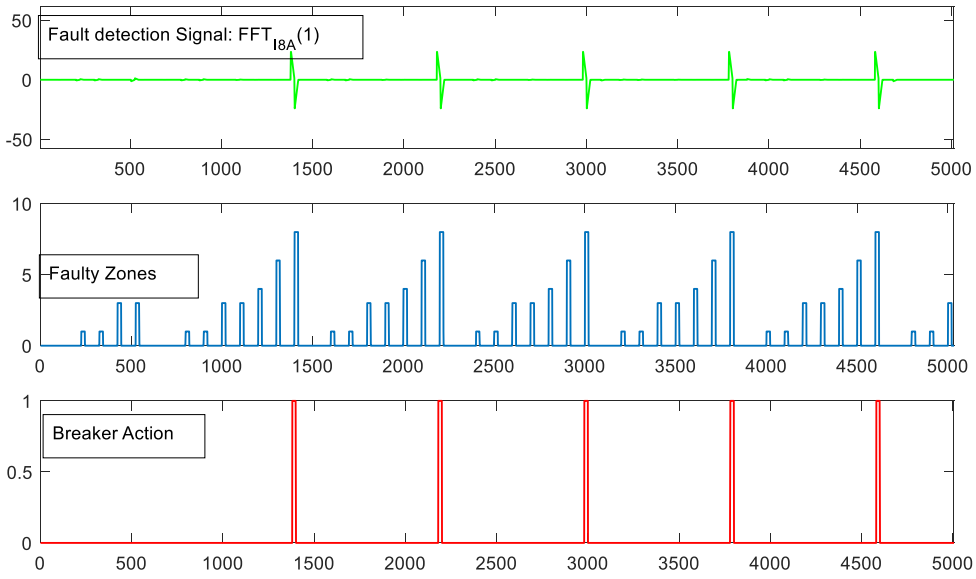

Figure 18. Fault detection signals and breaker action for a sequence of faults in Zone 8

The effectiveness of the method under different type of faults applied to the load in the test model is shown in Table 13. The method absolutely avoided erroneous detection and the undetected faults settle to a mere 0.75%. That is an exceptional achievement considering the fact that the test scenario includes faults of varying resistance. The only case where fee undetected faults were witnessed is the high impedance single line to ground fault. Comparison with a traditional over-

Preprints (www.preprints.org) | NOT PEER-REVIEWED | Posted: 30 March 2018 doi:10.20944/preprints201803.0272.v1

Peer-reviewed version available at Electronics 2018, 7, 61; doi:10.3390/electronics7050061

current protection of 125% relay setting reflects the exhibited improvement in fault detection accuracy by the method. The simple over-current protection setting values is assumed to take a value of 125% of the maximum load current under the non-fault test conditions.

Table 13. Performance of the Devised Method for different types of faults in Zone 8 (Load 2)

Type of Fault	Undetected			False detection		
	No. of points	Percentage Error (%)	Accuracy (%)	No. of points	Percentage Error (%)	Accuracy (%)
LG (Solid)	0	0.00	100.00	0	0.00	100.00
LG (HIF)	36	5.00	95.00	0	0.00	100.00
LLG (Solid)	0	0.00	100.00	0	0.00	100.00
LLG (HIF)	0	0.00	100.00	0	0.00	100.00
LL (Solid)	0	0.00	100.00	0	0.00	100.00
LL (HIF)	0	0.00	100.00	0	0.00	100.00
LLLG (Solid)	0	0.00	100.00	0	0.00	100.00
LLLG (HIF)	0	0.00	100.00	0	0.00	100.00
HIF	36	1.31	98.69	0	0.00	100.00
Solid	0	0.00	100.00	0	0.00	100.00
Total	36	0.75	99.25	0	0.00	100.00

Table 14. Performance of simple Over-current protection for faults in Zone 8 (Load protection)

Type of Fault	Undetected			False detection		
	No. of points	Percentage Error (%)	Accuracy (%)	No. of points	Percentage Error (%)	Accuracy (%)
LG (Solid)	0	0.00	100.00	0	0.00	100.00
LG (HIF)	720	100.00	0.00	0	0.00	100.00
LLG (Solid)	0	0.00	100.00	36	0.13	99.87
LLG (HIF)	665	100.00	0.00	0	0.00	100.00
LL (Solid)	665	100.00	0.00	0	0.00	100.00
LL (HIF)	684	100.00	0.00	0	0.00	100.00
LLLG (Solid)	684	100.00	0.00	0	0.00	100.00
LLLG (HIF)	684	100.00	0.00	0	0.00	100.00
HIF	2753	100.00	0.00	0	0.00	100.00
Solid	1349	66.36	33.64	36	0.04	99.96
Total	4102	85.71	14.29	36	0.02	99.98

As it can be seen from Table 14, the traditional over-current protection, with an exact opposite to the devised approach, showed poor performance. The special observation from this comparison is that the high impedance faults being completely unnoticed by the traditional over-current protection. That is due to the changes in load and generation during normal operation are considerably high and confused with the high impedance faults.

3.2. Island Mode

One of the challenges in microgrid protection is the lower effectiveness of the conventional approaches due to low fault current while the microgrid turns to island mode of operation. The following sets of tests are undertaken on the test microgrid model operating under island mode to evaluate whether the devised method can address this issue.

1. Fault in Zone 1 (Busbar Protection)
2. Fault in Zone 2 (Busbar protection)

Preprints (www.preprints.org) | NOT PEER-REVIEWED | Posted: 30 March 2018 doi:10.20944/preprints201803.0272.v1

Peer-reviewed version available at Electronics 2018, 7, 61; doi:10.3390/electronics7050061

3. Fault in Zone 4 (DER protection)
4. Fault in Zone 6 (Load protection)

3.2.1. Fault in Zone 1 (Busbar Protection)

The protection of this Busbar (BB1) is simplified due to withdrawal of the main feeder making the choice of the fault detection signal, which is the differential current, quit straight forward. The importance of the feature is, however, quantified and additional features are selected using the correlation analysis procedure in the same way as the protection of the other zones. The correlation analysis results, as shown in Table 14, showed that change in differential current is an immediate sign of fault occurring in the zone. Other features such as change in phase angle, magnitude of the first harmonic and the some of the detail wavelet energies of the bus voltage also showed significant correlation with the state of the concerned circuit breaker.

Table 14. Selection of most important features for Zone 1 (Busbar) protection – island mode

Rank	Corr	|Corr|	parameter
1	0.957	0.957	IDiff_BB1_RMS
2	-0.529	0.529	Ang_V1A
3	-0.407	0.407	ΔH_V1A(1)
4	-0.347	0.347	ΔEd_V1A(5)
5	-0.300	0.300	ΔEd_V1A(3)
6	-0.257	0.257	ΔNp_V1A
7	0.243	0.243	ΔEd_V1A(4)
8	0.227	0.227	ΔEa_V1A

The correlation between these selected fault detection signals and the state of the circuit breaker can also be affirmed from the graphical representation in Figure 19.

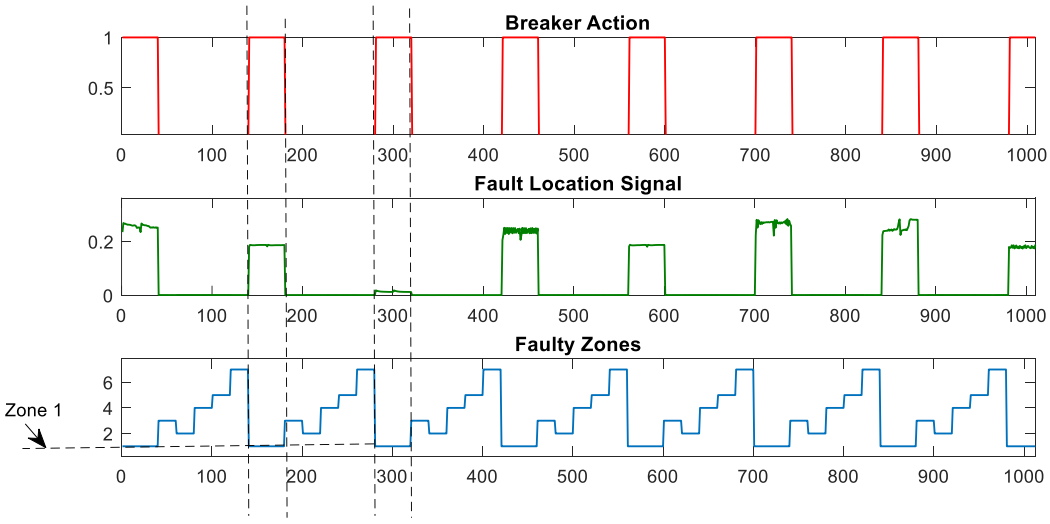

Figure 19. Fault detection signals and breaker action for a sequence of faults in Zone 8

The approach devised in this study is able to accurately identify all kinds of faults in Zone 1 with 100% accuracy. The result achieved though this technique is then compared to the use of conventional differential protection. As presented in Table 15, the devised approach is more effective than the conventional differential protection with most of the later failing to notice more than 8.89% of the faults, especially the HIFs.

Preprints (www.preprints.org) | NOT PEER-REVIEWED | Posted: 30 March 2018 doi:10.20944/preprints201803.0272.v1

Peer-reviewed version available at Electronics 2018, 7, 61; doi:10.3390/electronics7050061

Table 15. Comparing Devised approach with conventional differential protection for protection of for Zone 1 in island mode

		Devised Aproach	Conventional Diff.
Undetected	No. of points with confusion	0	512
	Total Events	5760	5760
	Percentage Error%	0.00	8.89
	Accuracy (%)	100.00	84.31
False detection	No. of points with confusion	0	0
	Total Events	111620	111620
	Percentage Error%	0	0
	Accuracy (%)	100	100

3.2.2. Fault in Zone 2 (Busbar protection)

The reason for performing additional testing for bus protection is because the first zone was made of just two branches and very simple. Zone 2 is a Busbar with more than two branches connected to it and can represent the case of Busbar protection better. The selected features for fault detection are not different from that of Zone 1 though their correlation is a little different this time (Table 16).

Table 15. Selection of most important features for Zone 2 (Busbar) protection – island mode

Rank	Corr	|Corr|	Parameter
1	0.958	0.958	IDiff_BB2_RMS
2	-0.298	0.298	Ang_V2A
3	-0.230	0.230	ΔH_V2A(1)
4	-0.196	0.196	ΔEd_V2A(5)
5	-0.169	0.169	ΔEd_V2A(3)
6	-0.145	0.145	ΔNp_V2A
7	0.136	0.136	ΔEd_V2A(4)
8	0.128	0.128	ΔEa_V2A

The method proved its effectiveness once again for protection of a bus bar in a microgrid under island mode with 100% accuracy. The method is also compared with and outperformed conventional approach of differential protection as shown in Table 16. Looking at the very high correlation between the differential current and the state of circuit breaker, one may suggest the solitary use this parameter should be enough. However, such a trial has rather consolidated the significance of the additional parameters as it can be seen from Table 16.

Table 16. Comparing Devised approach with conventional differential protection and option of using differential current as the only input for protection of for Zone 2 in island mode

		Devised Aproach	I_{Diff} only	Conventional Differential
Undetected	No. of points with confusion	0	26	193
	Total Events	2880	2880	2880
	Percentage Error (%)	0.00	0.90	6.70
	Accuracy (%)	100.00	99.10	93.30
False detection	No. of points with confusion	0	49	0
	Total Events	114500	114500	114500
	Percentage Error (%)	0	0.04	0
	Accuracy (%)	100	99.96	100

Preprints (www.preprints.org) | NOT PEER-REVIEWED | Posted: 30 March 2018 doi:10.20944/preprints201803.0272.v1

Peer-reviewed version available at Electronics 2018, 7, 61; doi:10.3390/electronics7050061

3.2.3. Fault in Zone 4 (DER protection)

For a microgrid operating in island mode, when a fault happed to DER1, the phase angle of the bus the current and the bus voltage are the most important parameters in addition to the other features listed in Table 17 from the wavelet and fast Fourier transforms.

Table 17. Selection of most important features for Zone 4 (DER) protection – island mode

Rank	Corr	|Corr|	parameter
1	-0.581	0.581	Ang__IDG1A
2	-0.297	0.297	Ang_VBB2_A
3	0.281	0.281	ΔH_IDG1A(1)
4	-0.230	0.230	ΔH_VBB2A(1)
5	-0.195	0.195	ΔEd_VBB2A(5)
6	-0.169	0.169	ΔEd_VBB2A(3)
7	-0.145	0.145	ΔNp_VBB2A
8	0.136	0.136	ΔEd_VBB2A(4)
9	0.128	0.128	ΔEa_VBB2A

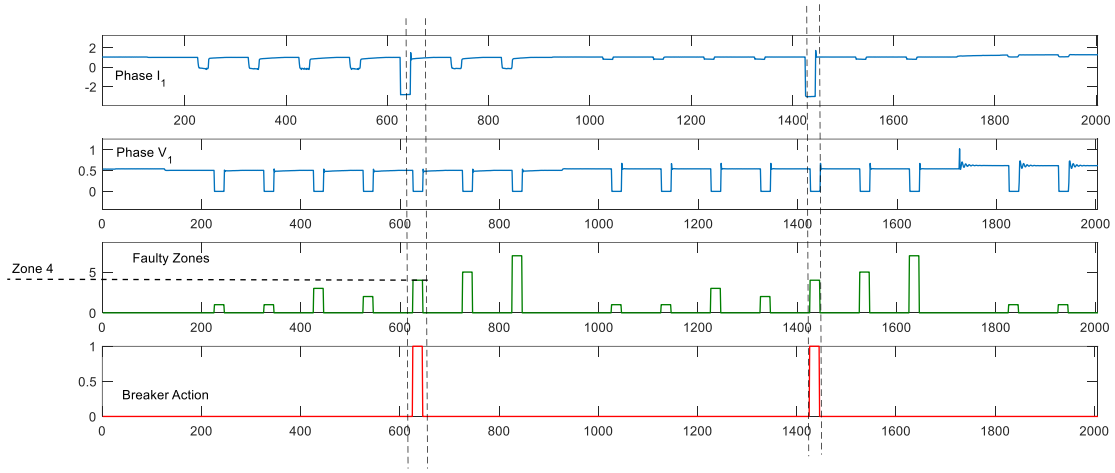

Figure 20. Changes in phase angle as important Fault detection signals for faults in Zone 4

The bagged decision tree based protection scheme with correlated input features extracted by winnowed FFT and WT resulted in fault detection accuracy of 97.92% with no single point mistakenly labeled as fault. The choice of the input sets was a critical factor for this very high accuracy as the use of phase angle of the branch current would only give an accuracy level of 47.05%.

3.2.4. Fault in Zone 6 (Load protection)

For a fault happening on zone 6 and Zone 7, where the U/f mode DER is either short circuited or faulted, the system will become completely unstable due to loose of a voltage and frequency reference. Hence, the correlation analysis result is extremely biased and less informative. The following features are selected as inputs based on the experience in the other zones and a common understanding.

Table 18. Selected Input features for Zone 6 (Load) protection – island mode

Selected input features for faults at Zone 6
Ang_Iload2
Ang_VBB3
Iload2_RMS
VBB3_RMS

The use of bagged decision trees trained with those inputs resulted in an efficient detection of different types of faults in the zone as shown in Table 19.

Table 19. Performance of Devised Approach for faults in Zone 6 (Load connected to same Busbar as U/f mode DER)

Parameter	Value
Undetected faults	186
Wrong detection	2880
Percentage Error (%)	6.458333
Accuracy	93.54167

4. Conclusions

With greater level of microgrid deployment in today's grid, their protection has become one of the mainstream research topics in the field. This study contributes to this field of research by recommending and verifying a novel bagged decision tree based protection scheme which makes systematic use of two of the most famous signal processing tools, fast Fourier and wavelet transform. The protection scheme devised in this study uses only local measurements, voltage of the bus bar in the protection zone and the current measurements from meters connected to the branches descended from the bus. Hence, the need for complex and time taking communication is avoided. The paper incorporates analysis of both current and voltage waveforms hence avoiding the issues related with current transformer saturation in current-only based methods.

After a list of candidate features extracted from windowed FFT and WT of the local voltage and current records is derived, the most important features were selected in a procedural manner though correlation analysis. The architecture of the bagged decision trees and the respective inputs were selected individually for the different protection zones. Rather than going to an absolutely theoretical proposition which is far from the industrial practice, upgrading the currently practical techniques with incorporation of the newly devised scheme is adopted in the study. Hence, the recommended approach was verified using a microgrid model initially modeled in PSCAD/EMTDS based on an operational microgrid and the results were compared to the conventional approaches such as differential, directional and overcurrent protections. In all the test cases, regardless of whether the microgrid is operating in either grid-connected or island modes or the faults being solid or high impedance faults, the devised approach showed great level of accuracy in detecting faults selectively both in terms of comparative and standard performance.

The signal features such as changes in magnitude of individual harmonics, phase angles, wavelet energy, number of peak values in the wavelet coefficients were very effective in signaling the presence of a fault in the different protection zones. Incorporation of the correlation analysis stage created a logical and objective way of input parameter selection whose effectiveness was as well reflected with the high level of accuracy achieved by the protection scheme as a whole. The use of bagged decision trees proved to be a coherent decision as substantial gains in fault detection accuracy were achieved. That is due to the de-correlation between the individual trees using different sets of inputs allowing for improved generalization and the high level of robustness by the technique with respect to noisy data.

Author Contributions: Solomon Netsanet contributed to the research model, data analysis techniques, implementation and writing of the paper. Jianhua Zhang and Dehua Zheng performed the supervision, professional advice and continuous follow-up of the study; all authors have read and approved the final manuscript.

Conflicts of Interest: The authors declare no conflict of interest

References

1. A. Hooshyar and R. Iravani, A New Directional Element for Microgrid Protection, *IEEE Transactions on Smart Grid* **2017**, *vol. PP, no. 99,* pp. 1-1. doi: 10.1109/TSG.2017.2727400
2. A. Hooshyar and R. Iravani, "Microgrid Protection," *Proceedings of the IEEE* **2017**, *vol. 105, no. 7*, pp. 1332-1353, doi: 10.1109/JPROC.2017.2669342
3. S. Ndjaba, G. T. Machnida, M. Nthontho, S. Chowdhury, S. P. Chowdhury and N. Mbuli, "Modeling and simulation of fault detection methods for power electronic interfaced microgrids," *47th International Universities Power Engineering Conference (UPEC)* **2012**, pp. 1-6. doi: 10.1109/UPEC.2012.6398556
4. Ricardo Escudero, Julien Noel, Jorge Elizondo, James Kirtley, Microgrid fault detection based on wavelet transformation and Park's vector approach, *Electric Power Systems Research* **2017**, Volume 152, pp 401-410, ISSN 0378-7796, https://doi.org/10.1016/j.epsr.2017.07.028.
5. H. Muda and P. Jena, "Superimposed Adaptive Sequence Current Based Microgrid Protection: A New Technique," in *IEEE Transactions on Power Delivery* **2017**, vol. 32, no. 2, pp. 757-767, doi: 10.1109/TPWRD.2016.2601921
6. Hare, J., Shi, X., Gupta, S., & Bazzi, A. Fault diagnostics in smart micro-grids: A survey. Renewable and Sustainable Energy Reviews **2016**, 60, 1114-1124
7. H. Al-Nasseri and M. A. Redfern, "Harmonics content based protection scheme for Micro-grids dominated by solid state converters," *12th International Middle-East Power System Conference*, 2008, pp. 50-56. doi: 10.1109/MEPCON.2008.4562361
8. K. Lai, M. S. Illindala and M. A. Haj-ahmed, "Comprehensive Protection Strategy for an Islanded Microgrid Using Intelligent Relays," in *IEEE Transactions on Industry Applications* **2017**, vol. 53, no. 1, pp. 47-55, doi: 10.1109/TIA.2016.2604203
9. S. Kar and S. R. Samantaray, "Time-frequency transform-based differential scheme for microgrid protection," in *IET Generation, Transmission & Distribution* **2014**, vol. 8, no. 2, pp. 310-320, doi: 10.1049/iet-gtd.2013.0180
10. A. Gururani, S. R. Mohanty and J. C. Mohanta, "Microgrid protection using Hilbert–Huang transform based-differential scheme," in *IET Generation, Transmission & Distribution* **2016**, vol. 10, no. 15, pp. 3707-3716, doi: 10.1049/iet-gtd.2015.1563
11. J. J. Q. Yu, Y. Hou, A. Y. S. Lam and V. O. K. Li, "Intelligent Fault Detection Scheme for Microgrids with Wavelet-based Deep Neural Networks," in *IEEE Transactions on Smart Grid* **2017**, vol. PP, no. 99, pp. 1-1. doi: 10.1109/TSG.2017.2776310
12. Parikh UB, Das B, Maheshwari R. Fault classification technique for series compensated transmission line using support vector machine. *Int J Electr Power Energy Syst* **2010**; vol 32, pp629–36.
13. Hadi Abdulwahid, A.; Wang, S. A Novel Approach for Microgrid Protection Based upon Combined ANFIS and Hilbert Space-Based Power Setting. *Energies* **2016**, *9*, 1042.
14. Hong, Y.-Y.; Wei, Y.-H.; Chang, Y.-R.; Lee, Y.-D.; Liu, P.-W. Fault Detection and Location by Static Switches in Microgrids Using Wavelet Transform and Adaptive Network-Based Fuzzy Inference System. *Energies* **2014**, *7*, 2658-2675.
15. D. P. Mishra, S. R. Samantaray and G. Joos, "A Combined Wavelet and Data-Mining Based Intelligent Protection Scheme for Microgrid," in *IEEE Transactions on Smart Grid* **2016**, vol. 7, no. 5, pp. 2295-2304, doi: 10.1109/TSG.2015.2487501
16. S. Kar, S. R. Samantaray and M. D. Zadeh, "Data-Mining Model Based Intelligent Differential Microgrid Protection Scheme," in *IEEE Systems Journal* **2017**, vol. 11, no. 2, pp. 1161-1169, doi: 10.1109/JSYST.2014.2380432
17. M. Kezunovic, "Advanced assessment of the power quality events," Ninth International Conference on Harmonics and Quality of Power. Proceedings (Cat. No.00EX441), Orlando, FL, 2000, pp. 834-839 vol.3. doi: 10.1109/ICHQP.2000.896837
18. L. Breiman, J. Friedman, C. J. Stone, and R. A. Olshen. Classiffcation and Regression Trees. Chapman and Hall/CRC, 1984.
19. Breiman, L. Machine Learning (2001) 45: 5. https://doi.org/10.1023/A:1010933404324
20. A. Criminisi, J. Shotton and E. Konukoglu. Decision Forests for Classification, Regression, Density Estimation, Manifold Learning and Semi-Supervised Learning. Microsoft Technical Report, MSR-TR-2011-114, 2011.
21. R. E. Schapire. The strength of weak learnability. Machine Learning, 5(2):197-227, 1990.